1   **DETERMINATION OF RENEWABLE ENERGY YIELD FROM MIXED WASTE**

2   **MATERIAL FROM THE USE OF NOVEL IMAGE ANALYSIS METHODS**

3

4   **S.T. Wagland [a]*, R. Dudley[b], M. Naftaly[b] and P.J. Longhurst [a]**

5

6   [a] Centre for Energy and Resource Technology, School of Applied Sciences, Cranfield

7   University, Cranfield, Bedfordshire, MK43 0AL, UK

8

9   [b] National Physical Laboratory, Teddington, Middlesex, TW11 0LW, UK

10   _____

11   * Corresponding author. Tel.: +44 (0) 1234 750111 extn 2404; Fax: +44 (0) 1234 751671

12   *E – mail address*: s.t.wagland@cranfield.ac.uk

13

14

Abstract

Two novel techniques are presented in this study which together promise to provide a system able to determine the renewable energy potential of mixed waste materials. An image analysis tool was applied to two waste samples prepared using known quantities of source-segregated recyclable materials. The technique was used to determine the composition of the wastes, where through the use of waste component properties the biogenic content of the samples was calculated. The percentage renewable energy determined by image analysis for each sample was accurate to within 5% of the actual values calculated. Microwave-based multiple-point imaging (AutoHarvest) was used to demonstrate the ability of such a technique to determine the moisture content of mixed samples. This proof-of-concept experiment was shown to produce moisture measurement accurate to within 10%. Overall, the image analysis tool was able to determine the renewable energy potential of the mixed samples, and the AutoHarvest should enable the net calorific value calculations through the provision of moisture content measurements. The proposed system is suitable for combustion facilities, and enables the operator to understand the renewable energy potential of the waste prior to combustion.

Keywords- Biogenic content, renewable energy, mixed wastes, image analysis, energy from waste

1. Introduction

The development of renewable energy technologies has become more prominent in recent years. This is due in part to European Union (EU) and global movement away from traditional energy generation from fossil fuels and the associated greenhouse gas (GHG) emissions (Del Río, 2011; Garg et al., 2009; Shafiullah et al., 2012; Tükenmez and Demireli, 2012), and also to the challenging target set by the European Union of producing 20% of electricity from renewable sources by 2020 (Council of the European Union, 2009; Lupa, 2011). Energy produced from biomass (Becidan et al., 2007; Defra, 2008; Mabee et al., 2011; Panoutsou et al., 2009; Qiao et al., 2011; Whittaker et al., 2011) and the bio-based fraction of wastes (Séverin et al., 2010; Velis et al., 2012; Wagland et al., 2011) presents a sustainable and secure solution to the renewable energy strategies.

Recovering value from waste materials is of key importance for the development of a sustainable future. Whilst the reuse, recovery and recycling of wastes is of interest, a significant proportion of residual waste remains that is either non-recoverable for various reasons, or has no commodity value. Therefore the thermal treatment of residual wastes is a management option that is popular across Europe, and is becoming more prominent in the UK as policy incentivises moving away from landfill disposal and towards the generation of renewable energy.

In Europe, national and international targets have been set up for waste recycling, recovery and diversion from landfill (Burnley et al., 2007), which in combination contribute to an integrated waste management system (Grosso et al., 2010). Likewise, existing targets regarding renewable energy production can include energy from biomass

1   and the biomass (or 'bio-based') fraction of waste (Wagland et al., 2011).   When

2   considering the mixed waste materials, it is critical to understand not only the biogenic

3   carbon content of the waste, but also the energy potential or yield from the bio-based

4   fraction. This is due to the renewable energy targets set (Council of the European Union,

5   2009), and the need to demonstrate the quantity of renewable energy generated from

6   mixed fuels in order to obtain any available financial incentives (such as the renewable

7   obligation certificates in the UK (Ofgem, 2009). Biogenic carbon is defined as the

8   fraction of total carbon present in a material that has been produced naturally by living

9   organisms, but not fossilised or fossil-derived (European Committee for Standardisation,

10   2007). A number of methods exist to determine the biogenic fraction of waste-derived

11   fuels, such as the manual-sorting and selective dissolution test methods (British standards

12   Institute, 2011c; Séverin et al., 2010), although the determination of ^{14}C by accelerated

13   mass spectrometry [AMS] is generally considered to be the most accurate (European

14   Committee for Standardisation, 2007; Fellner et al., 2007). However, these methods do

15   not link the biogenic fraction to the energy content of the sample.

16   One such approach in determining the biogenic content of a mixed waste material

17   would be by determining the physical composition of the mixed wastes, and then

18   matching each component to the biogenic carbon content, as determined by the ^{14}C

19   content. A novel test method has been recently developed by Wagland *et al.* (2012)

20   which can determine the composition of mixed wastes by a simple image analysis

21   technique (Wagland et al., 2012). This approach utilises Erdas Imagine™ v9.3 software

22   to process 12 mega pixel digital pictures by image correction and the placement of a dot-

23   grid over the image. The work described by Wagland *et al.* (2012) assesses a 1 m^2 area of

mixed waste; the density of each component is used together with the area covered by each component in order to calculate the percentage composition of the total waste material by weight. A very strong relationship was demonstrated between the hand sorted data and the results yielded by the image analysis method, with a mean correlation (r) of 0.91 ($p<0.05$) (Wagland et al., 2012).

The net calorific value (or 'lower heating value') of a fuel cannot be determined analytically, but is calculated from the gross calorific value ('higher heating value') and the content of moisture, carbon, hydrogen, oxygen and nitrogen (British Standards Institute, 2011a). However, the accurate determination of the net calorific value of the mixed waste requires an accurate measurement of moisture content across and through the waste volume. Optical technologies are not suitable for penetrating below the surface of the waste, and contact methods are difficult to implement in a waste processing environment. The most suitable non-contact technology for moisture measurement of the waste stream is the microwave moisture sensor: two such examples are the RadarTron 2550D (manufactured by ScaleTron) and Hydroprobe (manufactured by Hyronix). However, all currently available moisture sensors offer only single point measurement and provide a limited view of the moisture. This study presents a two-dimensional moisture imaging system, termed NPL AutoHarvest, under investigation for its application to waste moisture quantification with a spatial resolution close to one centimetre.

The image analysis tool is used to determine the composition and energy from the biogenic fraction of mixed wastes; the AutoHarvest technology is used to estimate the moisture content of waste samples. This study aims to demonstrate that the two

techniques can be combined to accurately determine the potential energy yield from the biogenic fraction of mixed wastes. The biogenic carbon content and the calorific values (gross and net) were determined for each individual component. The moisture content, determined throughout for each component, was used to adjust the net calorific value [NCV]. The NCV accounts for the latent heat of the water vapour formed by evaporation of the moisture within the waste and formed by the combustion of the hydrogen in the fuel. This latent heat is not recoverable in a conventional boiler plant. As such, the NCV represents the energy yield, representing the energy that would be produced in a 100% efficient non-condensing conversion process.

2. Methods

2.1. Waste materials and preparation

The waste components used in this study were gathered from materials collected from the Cranfield campus of Cranfield University. These included source-segregated components [paper, card, aluminium cans and dense plastic], film plastic, green waste, textiles, inert (rubble) and waste wood. The paper used was office paper, the card used was corrugated packaging cardboard, the dense plastics were PET bottles with a small fraction of HDPE lids, and the film plastics used were black bin bags. The textiles were a mixture of different clothing items and the waste wood was taken from pallets.

Each component was then 1) retained for image analysis; 2) dried and dispatched to the National Physical Laboratory [NPL] for microwave analysis for varying moisture content; and 3) dispatched to third party laboratories for analysis.

1   For the image analysis, the waste components were weighed before being

2   combined to produce two different batches, A and B, of mixed waste (42.7 and 45.5 kg

3   respectively). These batches were chosen to ensure that each waste sample was

4   sufficiently different: thus sample A did not include film plastic and inert; whilst sample

5   B did not include textiles. As a result of this selection and mixing, the composition of

6   each of these batches was known prior to image analysis.

7   Representative samples of the waste components (ca. 500 g) to be sent to NPL

8   were dried overnight in an oven at 50°C before being individually placed in air-tight

9   containers and delivered to NPL.

10   The waste components sent to the third party laboratories were not dried before

11   dispatch; they were however prepared by each respective laboratory in accordance with

12   the European standard method statement. Approximately 250 g of each component was

13   sent to Marchwood Scientific for proximate and ultimate analysis; whereas <50 g of each

14   component was used by Beta Analytic for biogenic carbon (^{14}C) analysis. Along with

15   efforts to ensure that the samples delivered to the third party laboratories were

16   representative of the whole batch, the components were analysed individually and were

17   typically the same type (i.e. PET bottles, office paper etc) and so variation was expected

18   to be minimal.

19

20   *2.2. Proximate, calorific value and biogenic analysis*

21   The moisture and ash content of the samples, along with the gross calorific values

22   [GCV], were analysed in accordance with the relevant standard methods (British

23   Standards Institute, 2011a, b; European Committee for Standardisation, 2010a) at

1 Marchwood Scientific [Southampton, England]. The net CV [NCV] was calculated from

2 the GCV as defined by the standard method (British Standards Institute, 2011a). GCV

3 analyses are within 5% repeatability, as is required by the standard methodology.

4 The biogenic carbon fraction was measured, calculated and reported for each

5 sample by Beta Analytic [London, England] in accordance with the accepted standard

6 methods (American Society for Testing Materials, 2012; European Committee for

7 Standardisation, 2007; International Organisation for Standardisation, 2013). The

8 technique used by Beta Analytic requires an accelerated mass spectrometer [AMS]. Here

9 the sample is combusted to form CO_2, which is then converted to graphite by passing

10 over a hot Fe catalyst with H_2. The graphite target is then bombarded by Caesium [Cs]

11 ions to release C ions. The rapid detection of $^{12}C^{4+}$, $^{13}C^{4+}$ and $^{14}C^{4+}$ ions allows for the

12 calculation of the ratio of ^{14}C to $^{12}C/^{13}C$ (European Committee for Standardisation, 2007).

13

14 *2.3. Image analysis*

15 Each of the two waste samples produced were spread evenly to represent a typical

16 conveyor belt as used to transport waste in treatment processing facilities. A 1 m^2

17 quadrant was placed over each part of the waste, and a digital image was captured of each

18 section. The quadrant was placed so as to ensure that all waste was covered during this

19 process, whilst avoiding overlap between sections.

20 The digital images were then processed using Erdas Imagine (v9.3) to crop and

21 geometrically correct the images before placing an 11x11 dot-grid over the image, as

22 described in a previous study (Wagland et al., 2012). Each dot covering each of the

1   waste component categories was manually selected, and the total number of dots covering

2   each component was counted digitally.

3   In the previous study (Wagland et al., 2012), individual components of fixed

4   volume (30 litres) were weighed to determine the density (g/cm^3) of each component

5   (European Committee for Standardisation, 2010b). However, errors were encountered

6   using this approach, and so in this study the individual components were spread out and

7   subjected to image analysis in order to calculate the mass per dot (kg/dot) for each

8   component. This accounts for the varying thickness of the waste layers, and reduces the

9   errors encountered during the conversion from number of dots to the % composition by

10   weight. The use of a calculated kg/dot over a number of samples (images) means that

11   variations in the thickness of the waste components are essentially averaged out.

12

13   *2.4. In-line moisture analysis*

14   The dielectric properties of water at microwave frequencies are well documented

15   (Ellison, 2007; Kaatze, 1989). Likewise, the use of microwaves for the measurement of

16   moisture content of materials has been known for some time (Kapilevich et al., 2007;

17   Meyer and Schilz, 1980; Sokoll and Jacob, 2007).

18   The absorption of a microwave beam by a material sample in air follows the Beer-

19   Lambert law (Hecht, 2001):

20

21                       $I_T = I_0 T e^{-\alpha d}$ **(1)**

22

Where I_T and I_0 are the transmitted and incident intensities respectively; α is the absorption coefficient, and d is the sample thickness. The coefficient T represents propagation loss at the interface, which may be due to a combination of reflection and scattering, and is dependent on both the angle of incidence and surface roughness. For a plane-parallel homogenous sample with faces that are smooth on the scale of the wavelength and which is positioned normal to the beam, scattering is absent, and T is given by the Fresnel formula (Hecht, 2001):

$$T = 1 - (n-1/n+1)^2 \qquad\qquad (2)$$

Where n is the refractive index of the sample material. When the above conditions are not met, the value of T will be reduced (except in the special case of Brewster-angle reflection (Hecht, 2001)). For a multi-component material, e.g. composite or containing water, the coefficient α must be replaced by $\alpha_1 C_1 + \alpha_2 C_2 + \alpha_3 C_3 + \dots$, where the subscripts refer to the individual components and C is the fractional concentration of each species.

Transmitted power loss in dB is calculated as:

$$Loss = -10 \log_{10} (I_T/I_0) = -4.34 \log_{10} T(\alpha d) \qquad\qquad (3)$$

and is additive when the beam passes through several material layers, i.e., for N layers:

$$Loss\ (N) = 4.34 \log_{10} (T_1 + T_2 + \dots T_N)\ (\alpha_1 d_1 + \alpha_2 d_2 + \dots A_N d_N) \qquad\qquad (4)$$

1   The microwave transmission loss of a mixed stack of materials, such as waste

2 stream, will therefore be determined by the absorptivity, thickness, orientation relative to

3 the beam, and texture of all individual layers in the stack.

4   The absorption coefficient α has a strong frequency dependence arising from

5 molecular resonances and phonon bands (Huang and Richert, 2008). This is particularly

6 true of liquid water, where absorption rises very steeply with frequency, as seen in Figure

7 1, which also shows the refractive index of water at relevant frequencies. At the

8 measurement frequency of 5 GHz α_{water} is 2.2 cm^{-1}. Since absorption increases with

9 frequency, selecting a higher frequency increases measurement sensitivity for low water

10 concentrations or for thin sample thickness. Microwave absorption coefficients of dry

11 wood, paper, plastic and fabric are much smaller than that of water (Simonis, 1982),

12 simplifying moisture content calculations. However, since the refractive index of water is

13 also much higher than that of most other waste materials, microwave transmission

14 through multiple layers of waste will also experience loss due to enhanced interface

15 reflection and refraction.

16

17   >>>>>>>>>>**Insert Figure 1**<<<<<<<<<<<<

18

19 **Figure 1.** The absorption coefficient and refractive index of liquid water at microwave
20 frequencies (Segelstein, 1981)
21

22   The moisture measurement system comprises a 5 GHz microwave transmitter and

23 receiver placed either side of the sample space and monitoring transmitted power. The

24 NPL AutoHarvest system utilises a linear array of 24 parallel receiving sensors,

producing a line image of loss distribution. A 2D loss map is generated by passing the
material through the sample space on a conveyor.

In order to evaluate the moisture content, the measured loss map must be
combined with the optical image analysis as described above. The loss of dry material
can then be estimated from the knowledge of material type and thickness; the difference
between measured loss and loss calculated for dry material would be attributable to the
presence of moisture. For a single layer of material, the effective thickness of the water in
the beam path can be calculated from:

$$Loss_{wet} - Loss_{dry} \cong -4.34 \log_{10} T_{dry} (\alpha_{water} d_{water}) \tag{5}$$

where the approximate sign is due to the fact that T will be different in wet and dry
materials, although the difference is not expected to be large: $T_{dry} \approx T_{wet}$.

In order to investigate the practical aspects of moisture measurements and to
produce some test calibration curves, a simple phantom was designed and its microwave
transmission measured using a single transmitter-receiver channel. The phantom was a 5
mm thick cellulose sponge, chosen for its high water retention capability and because
cellulose has similar microwave properties to a number of waste materials, such as paper,
cardboard, wood and natural-fibre textiles. Moisture content of the sponge was
determined by its weight. Figure 2 plots the measured microwave loss as a function of
sponge weight, and therefore moisture content, for three test frequencies: 5, 16 and 26
GHz. The weight of dry sponge was 0.7 g and its microwave loss was 0.2 dB at all test
frequencies. As expected from Equation 5, the relationship between loss and moisture

content is linear within measurement error. The scatter in the data is due largely to the

difficulty of ensuring a uniform distribution of water across the area of the sponge. It is

seen that at higher frequencies the slope is larger, due to increased water absorptivity.

Larger slope translates into higher measurements sensitivity. However, increased loss

requires larger signal-to-noise ratio in the measurement system: note that in Figure 2 the

noise in the data increases greatly when the loss exceeds 40 dB. Therefore the test

frequency must be selected with a view to a necessary trade-off between desired

measurement sensitivity and available signal-to-noise performance.

>>>>>>>>>>>**Figure 2**<<<<<<<<<<<<<<

Figure 2. Transmission loss as a function of weight of water in a test object (cellulose sponge),
measured at 5 GHz, 16 GHz, 26 GHz. Different symbols represent separate experimental runs.

The data indicates the scale of possible errors in measuring moisture content. It

may be expected that an uncertainty of ±2 dB is likely to be present in an industrial in-

line system, which would result in a corresponding uncertainly in water content of 17% at

5 GHz, 5% at 16 GHz, and 3% at 26 GHz.

Figure 2 demonstrates the type of calibration curves required to obtain reliable

moisture measurement from measured microwave loss. The imaging system must be

similarly calibrated for every type of material present in the waste stream, containing the

expected range of moisture levels. The material data will be combined with independent

measurements of thickness, or mass, of different types of materials. A statistical

algorithm can be developed that will estimate the microwave loss of dry material in a

1   mixed-waste stream as produced by the optical image analysis, compare it with the

2   measured loss, and evaluate the average moisture content of a volume of waste.

3

4   *2.5. Calculations*

5   To calculate the composition of each waste sample, the number of dots counted

6   for each component in each image was multiplied by the kg/dot as calculated previously,

7   to yield the mass (kg) of each component in each image. The sums of mass from each

8   image were then calculated to obtain the total weight of each component in the waste

9   sample, and were presented as weight-percentage composition (% w/w).

10   The biogenic carbon, GCV and NCV were calculated for each of the waste

11   samples from the determined composition using the weighted percentages. Subsequently,

12   the GCV and NCV from the biogenic fraction (GCV_{bio} and NCV_{bio}) were determined,

13   also using weighted averages.

14   The NCV at different moisture levels was calculated by rearranging the formula

15   provided in the standard method (British Standards Institute, 2011a), as shown in

16   Equation 6:

17

18   $Q_{p,net,m} = \{q_{v,gr,d} - 212.2 \times {}_w(H)_d - 0.8[{}_w(O)_d + {}_w(N)_d]\} \times (1 \times 0.01M) - 24.43M$ **(6)**

19

20   Where $Q_{p,net,m}$ is the NCV at constant pressure with moisture content (M), $q_{v,gr,d}$ is

21   GCV at constant volume on a dry basis. The hydrogen, oxygen and nitrogen content of

22   the moisture-free sample are shown as ${}_w(H/O/N)_d$.

14

1   By combining the elements in the curly brackets, a constant (k) was calculated for

2   each component relating to the elemental content. This essentially assumes that the H, O

3   and N content of each component remains consistent, however a previous study by

4   Chester *et al* (2008) demonstrated that the variation between the chemical composition of

5   waste components to be small (Chester et al., 2008). The equation was then adapted

6   accordingly to allow the calculation of NCV at specified moisture content, as shown in

7   Equation 7.

8

9        $$Q_{p,net,m} = (q_{v,gr,d} + k) \text{ x } (1 \text{ x } 0.01M) - 24.43M \tag{7}$$

10

11   The NCV at specified moisture content could then be calculated, demonstrating

12   how the moisture content measurements described previously would be applicable in

13   practice.

14   The energy from the biogenic fraction was calculated using the guideline method

15   from the Office for Gas and Electricity Markets [OFGEM] (Ofgem, 2011). However,

16   this guidance uses the assumed biogenic fractions as associated with the hand-sorting

17   method (British standards Institute, 2011c), meaning that waste fractions are 100%

18   biogenic (i.e. paper, card, wood etc.), 80% biogenic (leather and rubber), 50% (fabrics)

19   and 0% for plastics. These values are not accurate, and do not agree with laboratory

20   results published elsewhere (Fellner and Rechberger, 2009). Therefore, in this study the

21   OFGEM guidance has been modified to calculate the percentage biogenic energy from

22   the actual ^{14}C data for each waste component, which means that it is possible that certain

23   proportions of the energy from inherently biogenic materials (i.e. wood) is discounted.

3. Results and discussion

3.1. Waste sample properties

The proximate analysis, calorific values and biogenic fraction for each waste component is presented in Table 1 along with the composition of each waste mixture.

>>>>>>>>>>>>Insert Table 1<<<<<<<<<<<<<<<<

As shown in Table 1 the compositions of each of the prepared waste samples differ. Sample A contained significantly higher proportions of card, dense plastics and wood waste than sample B, and contained textiles but did not contain the inert material and film plastics used in sample B. The moisture content of the waste components varied as they were collected from source-segregated recyclables, and so some moisture was to be expected, especially in the garden waste. The GCV measured and NCV calculated for each component are similar to those reported in other studies (Burnley et al., 2011; Wagland et al., 2011), with the dense and film plastics yielding significantly higher energy content than the other components (Burnley et al., 2011).

The weighted average GCV and NCV for sample A for the composition shown in Table 1 were 14,600 and 13,600 kJ/kg respectively, and 9,980 and 9,280 kJ/kg respectively for sample B. Sample A has the higher energy content due to significantly greater proportions of card and wood, whereas sample B contains 26.4% inert material, which contributes zero energy value.

The biogenic fractions of the waste components generally vary based on the age of the material. As a part of the carbon cycle, ^{14}C is produced in the atmosphere (Marley et al., 2009) and can remain in the atmosphere for a significant period of time prior to uptake from biomass material. The half-life of ^{14}C is 5,730 years (European Committee for Standardisation, 2007; Marley et al., 2009), and so the biogenic content of wood, garden waste and paper is lower than 100% due to the partial decay of ^{14}C. Measured biogenic carbon content of wood-derived materials can be explained if the wood was sourced from a relatively old tree; the wood was taken from the centre-rings of a long-lived tree or if the wood was partially contaminated with petrochemical components (paint, oils or varnish). The biogenic content of card was higher than that of paper and wood, despite also being of woody origin. This is likely to be due to the card being produced from much younger woodlands, as occurs in practices of sustainable forestry. It is also likely that the card used in this study was produced from virgin materials, whereas the paper may have been recycled several times before. It is documented that the precision of the ^{14}C technique is 2% relative standard deviation [RSD] for values between 10-100% biogenic carbon content (European Committee for Standardisation, 2007).

Plastic is of petrochemical origin, and so it would be expected that the biogenic content would be 0%, however some biogenic material was measured. This could be an error in the analysis as the precision of the ^{14}C technique is quoted as 5% relative standard deviation [RSD] between for values of 0-10% biogenic carbon content (European Committee for Standardisation, 2007). Otherwise, it is possible that a very small proportion of the plastics used in this study were produced from bio-based polymers (bio-plastics).

3.2. Image analysis

The results of the image analysis for each of the two samples are shown in Table 2, highlighting the weight of each component determined by this technique and the percentage composition.

>>>>>>>>>>>>>>>>Insert Table 2<<<<<<<<<<<<<<<<<

The weighted average GCV and NCV for the composition determined by image analysis, as shown in Table 2, were 14,900 and 13,800 kJ/kg respectively for sample A and 9,460 and 8,800 kJ/kg respectively for sample B. These are very close to the weighted average GCV and NCVs reported for the prepared samples (Table 1), which is due to the accuracy of the composition obtained (or recorded) by image analysis for both samples.

It is clearly seen in Table 2 that the image analysis technique over-estimates the weight of each component in most cases, with wood and garden waste in sample B being exceptions. These errors are likely to be due in part to the variations in sample thickness; this is a limitation of the method that requires further consideration and investigation. Whilst the weights are over-estimated, they are done so proportionately. This is shown by the very strong correlations (r = 0.992 and 0.988 for sample A and B respectively). Likewise there is also a very strong correlation (r = 0.993 and 0.988 for samples A and B respectively) between the percentage composition of the prepared waste sampled and the values determined by image analysis. The significance of these correlations are $p < 0.005$ for each case.

The differences between the known mass of the waste components and their determined mass are due to the translation of dot count to weight. As a result, the conversion used requires careful consideration, as this error is likely to be more pronounced in waste samples of much greater depth where overlap and hidden components are expected. The impact of greater depth could be minimised by measuring the depth of the waste, or by controlling the depth by ensuring that the samples are more spread out and do not exceed a certain height. As a waste sampling tool, the image analysis method is not suitable in its current form for monitoring the mass of waste components. However, this method is evidently highly suited for measuring the percentage composition as shown by the very strong correlation.

3.3. Microwave image analysis

Utilising the microwave imaging system, samples of the supplied waste types were imaged on a mock conveyor, as shown in Figure 3.

>>>>>>>>>>>>Insert Figure 3<<<<<<<<<<<<<<<

Figure 3. Mock conveyor belt set-up (a) samples ready to be analysed, (b) microwave image of dry samples, and (c) microwave image of wet samples. Lighter shades represent higher absorption.

Textile, wood, paper and plastic were measured before and after being sprayed with water, which increased the total weight of the four samples by 30%. The contrast in microwave images results from differential microwave absorption, higher absorption being displayed as white. In Figure 3b and 3c, the wood sample exhibits stronger absorption compared with the other three samples, due to its greater absorptivity,

1   thickness and density, and also due to some trapped moisture. However, after spraying

2   with water the textile sample becomes the most highly absorbing as a result of its large

3   water retention capacity. In contrast, in the wood, paper and plastic samples water

4   remained on or close to the primary sprayed surface, with little moisture penetration into

5   the body of the material, therefore producing a weaker effect on microwave absorption.

6   Moisture content of different materials was evaluated, the results being

7   summarised in Table 3. The thickness of the water layer in the beam path was estimated

8   by weighing the material before and after spraying and dividing the weight difference by

9   the sample area. The microwave loss due to water was then measured as the difference in

10   loss between dry and wet samples, and the thickness of the water layer was calculated

11   from Equation 5.

12   >>>>>>>>>>>>>>**Insert Table 3**<<<<<<<<<<<<<<<<<<

13

14   It is seen that in the case of fabric the moisture content measured from microwave

15   loss agrees with that derived from weighing the material; the case of cardboard is

16   borderline, in that the obtained value is similar to the uncertainty; whilst wood is below

17   the detection threshold of the system.

18   The results in Table 3 demonstrate the feasibility of microwave moisture

19   detection, as well as highlight the requirements for system performance and the detection

20   limits. The present system, which has a loss measurement uncertainty of 0.2 dB is

21   incapable of detecting a compound water layer of less than 0.05 mm. In an industrial

22   environment additional measurement errors may arise from the deployment and operation

23   of the system, and must be addressed by careful system design and data analysis.

1 Nevertheless, further development of the microwave imaging technology should enable

2 the average moisture content to be measured with an accuracy of better than 10 %,

3 offering a viable solution for the waste industry.

4

5 *3.4. Renewable energy content*

6 The renewable energy values, as a percentage of the total GCV and NCV, as

7 calculated from the known composition of the waste samples and the composition

8 determined by the image analysis method, are presented in Table 4.

9

10 >>>>>>>>>>>>**Insert Table 4**<<<<<<<<<<<<<<

11

12 As shown in Table 4, the renewable GCV and NCV, as a percentage of the total

13 (shown in Tables 1 and 2), calculated from the known composition and from the image

14 analysis-derived composition, were lower for sample A than for sample B. This is due to

15 the significantly greater proportion of dense plastic in sample A, which contributed to a

16 large fraction of the total energy content but was only 1% biogenic from the ^{14}C analysis.

17 The percentage renewable energy determined by image analysis was lower than values

18 calculated from the known sample mixtures; however these are still very similar (within

19 5% of the actual values, as shown in Table 4).

20 It is important to understand the impact of the moisture content on the NCV, as

21 whilst the overall moisture content of the sample is a key consideration, the moisture

22 retention, or specific load, for each component varies (Velis et al., 2012). Therefore, the

23 ability of the AutoHarvest system to monitor moisture content at multiple points is a key

21

characteristic of the proposed system. Using Equation 7, the NCV of each waste

component used was calculated at a range of moisture content (Figure 4).

>>>>>>>>>>>>>>**Figure 4**<<<<<<<<<<<<<<<

Figure 4. The NCV of each waste component at different moisture content (calculated

from Equation 7).

As seen in Figure 4, the NCV falls with increasing moisture content. Notably, the

decrease is steeper for plastic than for natural-source materials such as paper, textiles and

wood. Nevertheless, even for the latter, the NCV decreases by a factor of 3 for a moisture

content of around 60%. Figure 4 therefore highlights the strong negative impact of

moisture on energy recovery.

The biogenic fraction of the prepared samples was higher than that of typical

mixed wastes, as shown in a previous study (Fellner and Rechberger, 2009) where the

average biogenic fraction of mixed household waste and mixed commercial wastes were

70.3 and 64.2% respectively. As the biogenic fraction of mixed wastes is reported to

yield lower energy than the non-biogenic fractions due to the oxygenation of the Carbon

within the fuel (Voong and Othen, 2007), the energy from the biogenic fraction will be

lower than the biogenic proportion.

Whilst the recovery of recyclable materials such as paper, card, metals and

plastics increases, there will be a remaining residual waste stream for the foreseeable

future. As such, residual waste has an important role to play in the recovery of renewable

energy as EU member states strive towards the 20% of electricity generated from

renewable sources by 2020. As the residual waste stream changes with time, due to the

removal of recyclable materials, the composition as well as the total available volume

will change. Further work is required to estimate the potential impacts of future recycling

on the renewable energy content of residual wastes (MSW and C&I). Furthermore,

consideration needs to be given to the future uptake of plastics derived from bio-based

materials, which are becoming increasingly common as alternatives to fossil-based

plastics (Eerhart et al., 2012).

The Cranfield-NPL system is suitable for thermal energy recovery systems such

as combustion, gasification and pyrolysis. This system can (or may) certainly be of use at

waste processing facilities which produce a refuse-derived fuel [RDF] /solid recovered

fuel [SRF] as a commodity sold to a third party for use elsewhere. The properties of the

product, in this case the % NCV_{bio} (i.e. the ROC eligibility), could be determined prior to

dispatch, thus potentially enabling a more dynamic market for the material, with the

specific grade and value of the SRF being known for each batch produced.   Further

investigation of the proposed system in a waste processing environment would be

required to ascertain parameters such as the number of required samples, the conveyor

belt speed and sample thickness control.   A schematic for the proposed system in a waste

processing environment is provided in Figure 5, indicating potential height sensors which

would enable corrections on sample thickness.

>>>>>>>>>>>>>**Insert Figure 5**<<<<<<<<<<<<<<<<

23

Figure 5. Schematic of proposed system on a conveyor belt.

The conversion of waste components to liquid and/or gaseous fuels (as with gasification and pyrolysis) is not as straightforward as regards the CV, as used in this study. Therefore further consideration would be required. Ofgem has recently suggested that a method of assessing energy produced from biomass-derived material by a gasification process can be adopted by measuring the ^{14}C ratio within CO_2 in the flue gas (Ofgem, 2011). This method is appropriate for combustion; however for gasification this may not be directly applicable.

4. Conclusions

The two image analysis tools presented each demonstrate the potential to be applied, combined in a single system, for estimating the renewable energy potential of mixed wastes in a thermal treatment facility. The proposed system would, however, only be applicable to conventional incineration/combustion processes due to the more complex chemical processes involved in advanced thermal conversion technologies such as gasification or pyrolysis.

Alternative applications would be for the determination of mixed waste composition as outlined in a previous study by Wagland *et al.* (2012), or for the certification of SRF prior to delivery to an end-user.

24

References

American Society for Testing Materials, 2012. ASTM D6866-12 Standard test methods for determining the biobased content of solid, liquid, and gaseous samples using radiocarbon analysis.

Becidan, M., Varhegyi, G., Hustad, J.E., Skreiberg, O., 2007. Thermal Decomposition of Biomass Wastes. A Kinetic Study. Industrial & Engineering Chemistry Research 46, 2428-2437.

British Standards Institute, 2011a. BS EN 15400:2011, Solid recovered fuels. Determination of calorific value.

British standards Institute, 2011b. BS EN 15403:2011, Solid recovered fuels. Determination of ash content.

British standards Institute, 2011c. BS EN 15440:2011, Solid recovered fuels. Methods for the determination of biomass content.

Burnley, S., Phillips, R., Coleman, T., Rampling, T., 2011. Energy implications of the thermal recovery of biodegradable municipal waste materials in the United Kingdom. Waste Management 31, 1949-1959.

Burnley, S.J., Ellis, J.C., Flowerdew, R., Poll, A.J., Prosser, H., 2007. Assessing the composition of municipal solid waste in Wales. Resources, Conservation and Recycling 49, 264-283.

Chester, M., Stupples, D., Lees, M., 2008. A comparison of the physical and chemical composition of the UK waste streams based on hypothetical compound structure, Proceedings 13th European Biosolids and Organic Resources, Manchester, UK.

Council of the European Union, 2009. Directive 2009/28/EC on the promotion of the use of energy from renewable sources Official Journal of the European Communities L 140/52.

Defra, 2008. Wood waste as a biomass fuel. Defra.

Del Río, P., 2011. Analysing future trends of renewable electricity in the EU in a low-carbon context. Renewable and Sustainable Energy Reviews 15, 2520-2533.

Eerhart, A.J.J.E., Faaij, A.P.C., Patel, M.K., 2012. Replacing fossil based PET with biobased PEF; Process analysis, energy and GHG balance. Energy and Environmental Science 5, 6407-6422.

Ellison, W.J., 2007. Permittivity of Pure Water, at Standard Atmospheric Pressure, over the Frequency Range 0--25 THz and the Temperature Range 0--100 [degree]C. Journal of Physical and Chemical Reference Data 36, 1-18.

European Committee for Standardisation, 2007. PD CEN/TS 15591:2007, Solid recovered fuels. Determination of the biomass content based on the ^{14}C method.

European Committee for Standardisation, 2010a. CEN/TS 15414-2:2010, Solid recovered fuels. Determination of moisture content using the oven dry method. Determination of total moisture content by a simplified method.

European Committee for Standardisation, 2010b. DD CEN 15401, Solid recovered fuels. Determination of bulk density.

1 Fellner, J., Cencic, O., Rechberger, H., 2007. A new method to determine the ratio of electricity
2 production from fossil and biogenic sources in waste-to-energy plants. Environ. Sci. Technol. 41,
3 2579-2586.
4 Fellner, J., Rechberger, H., 2009. Abundance of 14C in biomass fractions of wastes and solid
5 recovered fuels. Waste Management 29, 1495-1503.
6 Garg, A., Smith, R., Hill, D., Longhurst, P.J., Pollard, S.J.T., Simms, N.J., 2009. An integrated
7 appraisal of energy recovery options in the United Kingdom using solid recovered fuel derived
8 from municipal solid waste. Waste Management 29, 2289-2297.
9 Grosso, M., Motta, A., Rigamonti, L., 2010. Efficiency of energy recovery from waste
10 incineration, in the light of the new Waste Framework Directive. Waste Management 30, 1238-
11 1243.
12 Hecht, E., 2001. Optics, 4th ed. Addison Wesley.
13 Huang, W., Richert, R., 2008. The physics of heating by time-dependent fields: microwaves and
14 water revisited. Journal of Physical Chemistry B 112, 9909-9913.
15 International Organisation for Standardisation, 2013. ISO 13833:2013, Stationary source
16 emissions- determination of the ratio of biomass (biogenic) and fossil-derived carbon dioxide:
17 radiocarbon sampling and determination.
18 Kaatze, U., 1989. Complex permittivity of water as a function of frequency and temperature.
19 Journal of Chemical and Engineering Data® 34, 371-374.
20 Kapilevich, B., Litvak, B., Wainstein, V., Moshe, D., 2007. Density-independent moisture
21 measurements of polymer powders using a mm-wave quasi-optical resonator. Measurement
22 Science and Technology 18, 1069-1073.
23 Lupa, C.J., 2011. Energy from waste in the United Kingdom, International Sustainable Energy
24 Review, pp. 30-33.
25 Mabee, W.E., McFarlane, P.N., Saddler, J.N., 2011. Biomass availability for lignocellulosic ethanol
26 production. Biomass and Bioenergy 35, 4519-4529.
27 Marley, N.A., Gaffney, J.S., Tackett, M., Sturchio, N.C., Heraty, L., Martinez, N., Hardy, K.D.,
28 Marchany-Rivera, A., Guilderson, T., MacMillan, A., Steelman, K., 2009. The impact of biogenic
29 carbon sources on aerosol absorption in Mexico City. Atmospheric Chemistry and Physics 9,
30 1537-1549.
31 Meyer, W., Schilz, W., 1980. A microwave method for density independent determination of the
32 moisture content of solids. Journal of Physics D: Applied Physics 13, 1823-1830.
33 Ofgem, 2009. Renewables Obligation: fuel measurement and sampling guidance. Ofgem,
34 London.
35 Ofgem, 2011. Renewables obligation: fuel measurement and sampling guidance, in: Renewables
36 and CHP (Ed.). Ofgem, London.
37 Panoutsou, C., Eleftheriadis, J., Nikolaou, A., 2009. Biomass supply in EU27 from 2010 to 2030.
38 Energy Policy 37, 5675-5686.
39 Qiao, W., Yan, X., Ye, J., Sun, Y., Wang, W., Zhang, Z., 2011. Evaluation of biogas production from
40 different biomass wastes with/without hydrothermal pretreatment. Renewable Energy 36,
41 3313-3318.
42 Segelstein, D.J., 1981. The complex refractive index of water (M.Sc Thesis), Department of
43 Physics. University of Missouri, Kansas City.
44 Séverin, M., Velis, C.A., Longhurst, P.J., Pollard, S.J.T., 2010. The biogenic content of process
45 streams from mechanical-biological treatment plants producing solid recovered fuel. Do the
46 manual sorting and selective dissolution determination methods correlate? Waste Management
47 30, 1171-1182.

1 Shafiullah, G.M., Amanullah, M.T.O., Shawkat Ali, A.B.M., Jarvis, D., Wolfs, P., 2012. Prospects of
2 renewable energy - a feasibility study in the Australian context. Renewable Energy 39, 183-197.
3 Simonis, G.J., 1982. Index to the literature dealing with the near-millimeter wave properties of
4 materials. International Journal of Infrared and Millimeter Waves 3, 439-469.
5 Sokoll, T., Jacob, A.F., 2007. In-situ moisture detection system with a vector network analyser.
6 Measurement Science and Technology 18, 1088-1093.
7 Tükenmez, M., Demireli, E., 2012. Renewable energy policy in Turkey with the new legal
8 regulations. Renewable Energy 39, 1-9.
9 Velis, C., Wagland, S., Longhurst, P., Robson, B., Sinfield, K., Wise, S., Pollard, S., 2012. Solid
10 Recovered Fuel: Influence of Waste Stream Composition and Processing on Chlorine Content
11 and Fuel Quality. Environ. Sci. Technol. 46, 1923-1931.
12 Voong, D., Othen, S., 2007. C14 analysis of biomass energy content - description of method.
13 Fichtner.
14 Wagland, S.T., Kilgallon, P., Coveney, R., Garg, A., Smith, R., Longhurst, P.J., Pollard, S.J.T.,
15 Simms, N., 2011. Comparison of coal/solid recovered fuel (SRF) with coal/refuse derived fuel
16 (RDF) in a fluidised bed reactor. Waste Management 31, 1176-1183.
17 Wagland, S.T., Veltre, F., Longhurst, P.J., 2012. Development of an image-based analysis method
18 to determine the physical composition of a mixed waste material. Waste Management 32, 245-
19 248.
20 Whittaker, C., Mortimer, N., Murphy, R., Matthews, R., 2011. Energy and greenhouse gas
21 balance of the use of forest residues for bioenergy production in the UK. Biomass and Bioenergy
22 35, 4581-4594.

23

24

slope:
@ 5 GHz = 0.39±0.01 dB/g
@ 16 GHz = 1.31±0.03 dB/g
@ 26 GHz = 2.30±0.07 dB/g
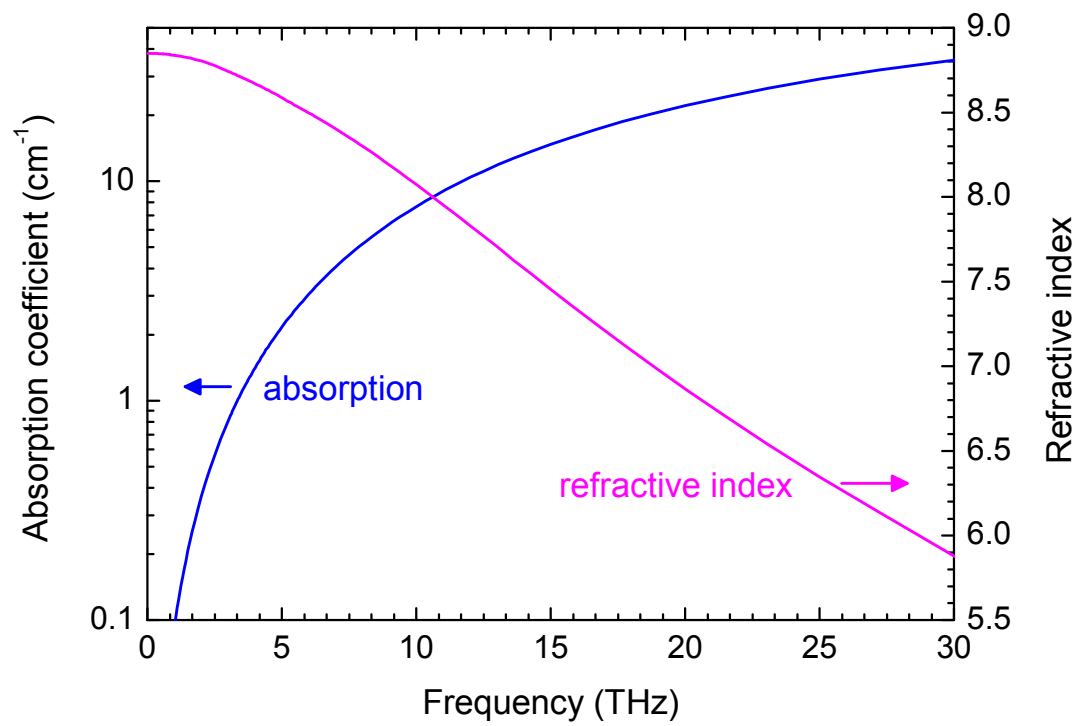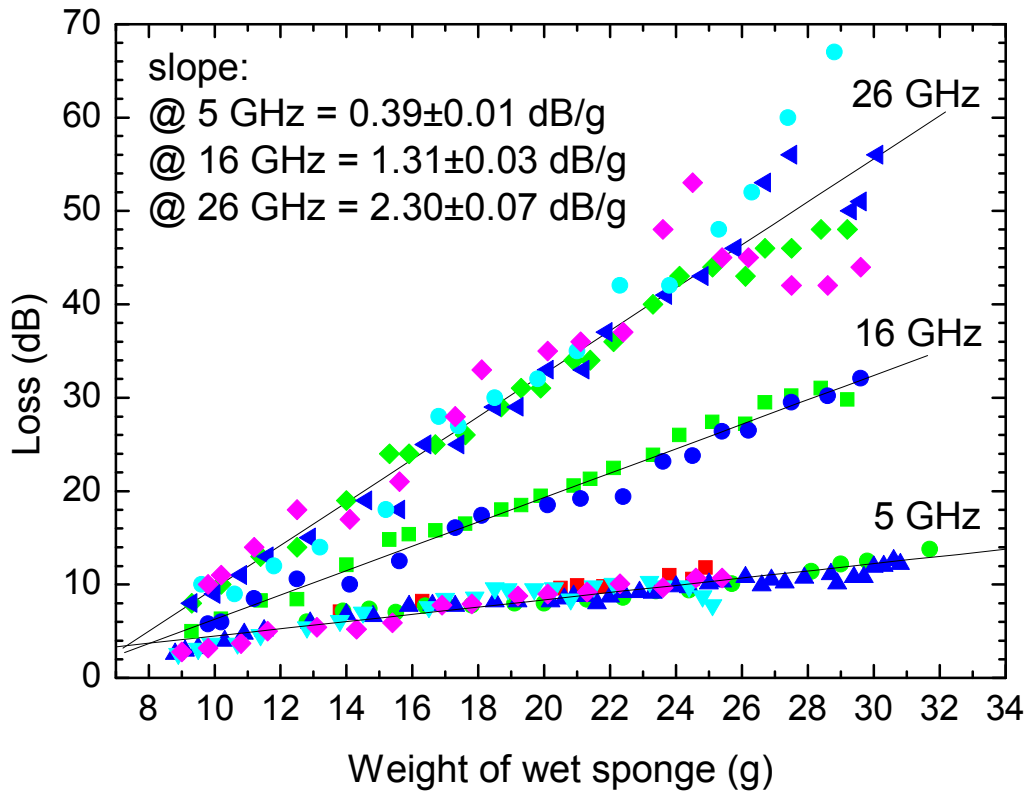
(a)
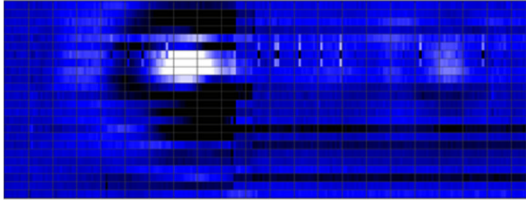
(b)
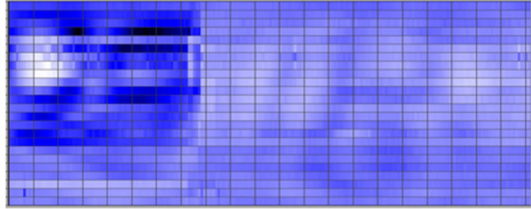
(c)
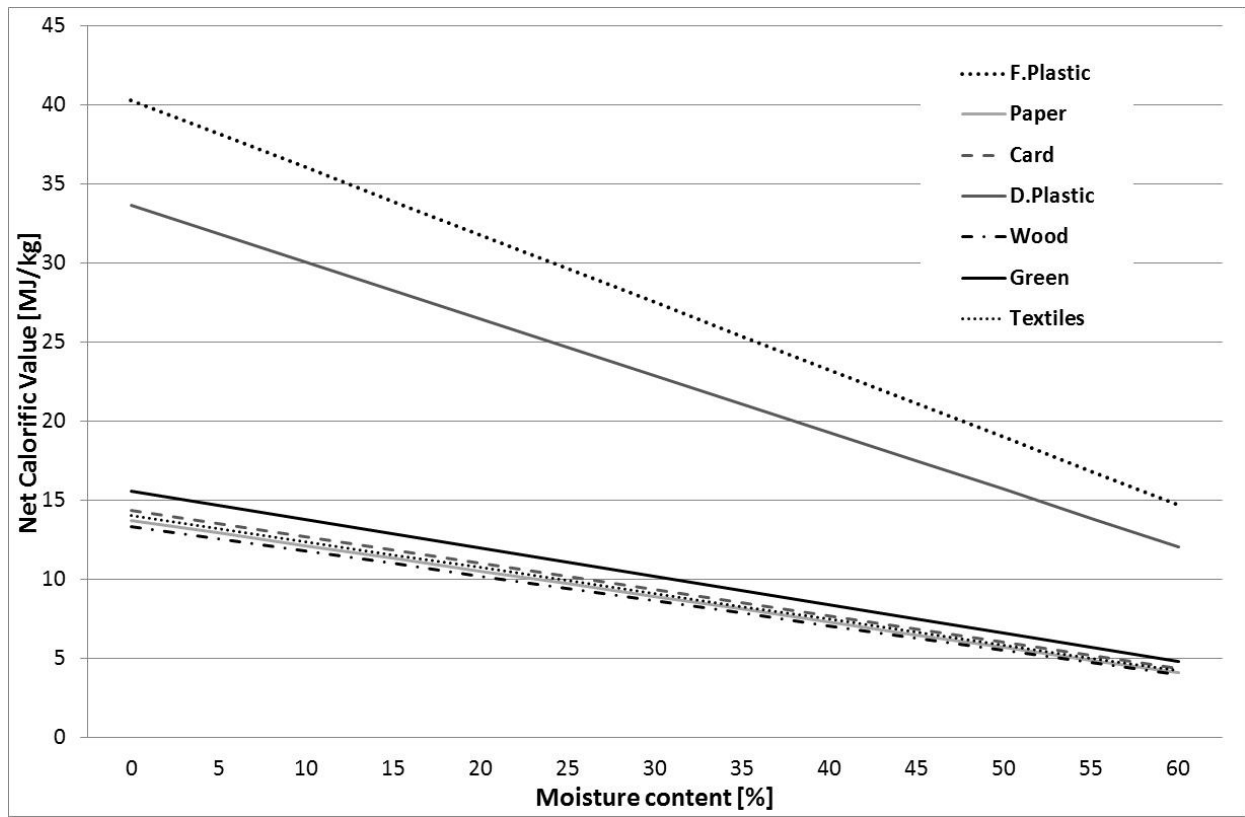
Figure 5
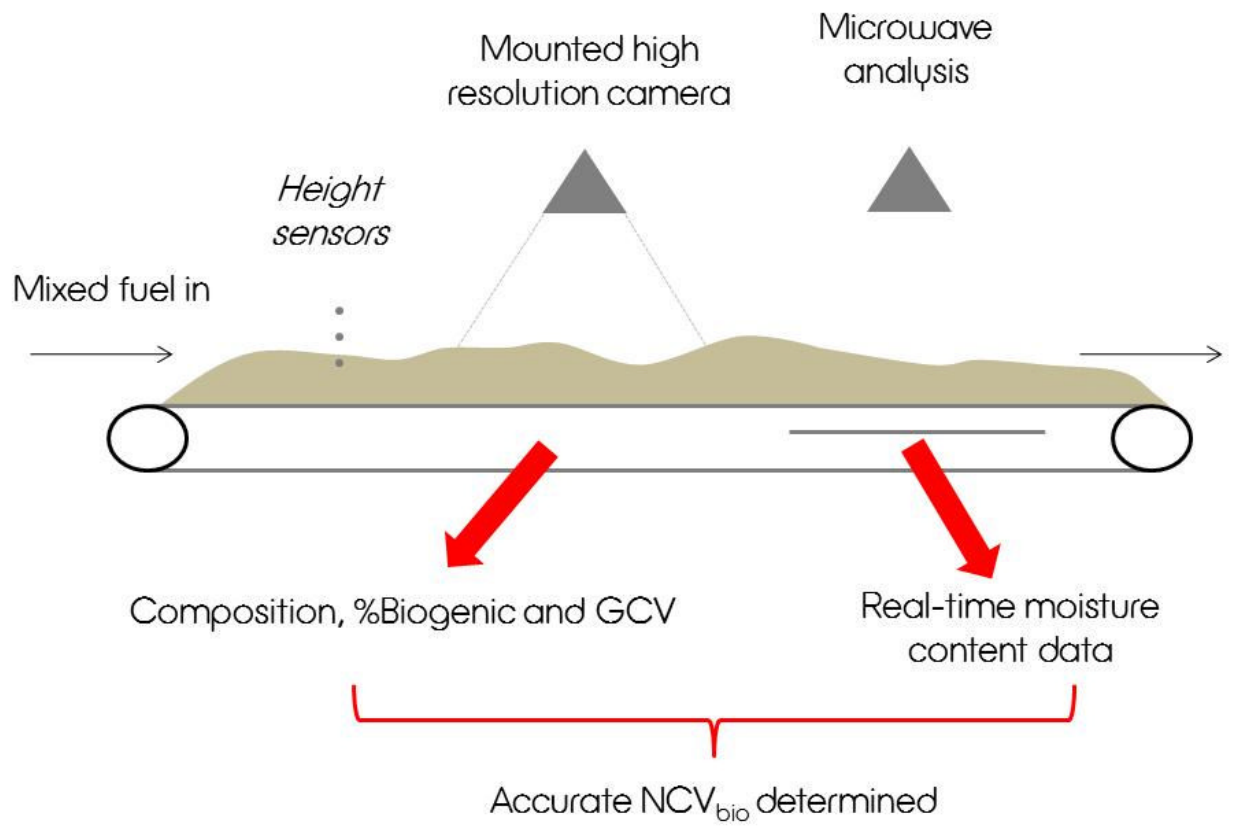
Component	Weight (kg)		% Composition		Ash (%)	Moisture (%)	Gross CV [MJ/kg]	Net CV [MJ/kg]	Biogenic C (%)
	A	B	A	B					
Paper	11.9	17.5	27.9	38.5	0.3	7.2	13,500	12,600	94
Card	12.9	3.6	30.2	7.9	1.2	13.9	13,000	12,100	100
D.Plastic	4.6	1.4	10.8	3.1	0.1	1.6	29,200	27,200	1
F.Plastic	-	0.5	-	1.1	5.4	2.9	41,300	39,100	1
Metal	1.0	1.8	2.3	4.0	-	-	-	-	-
Garden waste	3.4	4.5	8.0	9.8	2.3	25.8	11,800	11,000	96
Textiles	2.2	-	5.2	-	3	6.2	14,000	13,000	86
Wood	6.7	4.2	15.7	9.2	2.4	9.8	13,200	12,300	90
Inert	-	12	-	26.4	-	-	-	-	-
Total	**42.7**	**45.5**							

Table 1. Proximate, calorific, ^{14}C and composition data for mixed waste materials.

Component	Weight (kg)		% Composition	
	A	B	A	B
Paper	19.6	23.4	25.7	38.9
Card	20.9	5.4	27.4	9.0
D.Plastic	10.0	1.8	13.1	2.9
F.Plastic	-	0.8	-	1.3
Metal	2.1	2.2	2.8	3.7
Garden waste	6.7	4.1	8.8	6.8
Textiles	4.1	-	5.4	-
Wood	12.9	3.8	16.9	6.3
Inert	-	18.7	-	31.0
Total	**76.4**	**60.2**		
Correlation (r)	**0.992**	**0.988**	**0.993**	**0.988**

Table 2. Component weight and % composition determined by image analysis

Material	Thickness of water layer (mm)	Loss when dry (dB)	Loss when wet (dB)	Loss due to water (dB)	Calculated thickness of water (mm)
Wood	0.006±0.001	3.5±0.2	3.6±0.2	0.1±0.3	0.02±0.08
Cardboard	0.033±0.002	0.1±0.2	0.3±0.2	0.2±0.3	0.05±0.08
Fabric	0.33±0.01	0.3±0.2	1.6±0.2	1.3±0.3	0.31±0.07

Table 3. Moisture content of different materials calculated from microwave loss.

		Renewable gross CV [MJ/kg]	Renewable net CV [MJ/kg]
Component	Paper	12,700	11,800
	Card	13,000	12,100
	D.Plastic	292	272
	F.Plastic	413	391
	Metal	-	-
	Garden waste	11,300	10,500
	Textiles	12,000	11,200
	Wood	11,900	11,100
	Inert	-	-
% Renewable energy	Sample A	**74.69**	**74.69**
	Image analysis Sample A	**70.72**	**70.71**
	Sample B	**80.25**	**80.09**
	Image analysis Sample B	**79.61**	**79.44**

Table 4. % renewable energy from each waste sample, determined from the known composition and from image analysis. CVs quoted on an 'as received' basis.